

## Synthesis of the Rheb and K-Ras4B GTPases\*\*

Yong-Xiang Chen, Sebastian Koch, Katharina Uhlenbrock, Katrin Weise, Debapratim Das, Lothar Gremer, Luc Brunsveld, Alfred Wittinghofer, Roland Winter, Gemma Triola, and Herbert Waldmann\*

Dedicated to Prof. Horst Kunz on the occasion of his 70th birthday.

Small GTPases of the Ras superfamily critically regulate numerous cellular programs and are involved in the establishment of disease, in particular cancer.<sup>[1]</sup> Two relevant examples are the K-Ras4B protein and the Ras homologue enriched in brain (Rheb) protein. Rheb activates the mTORC1 (mammalian target of rapamycin complex 1) signaling pathway, which plays a central role in regulating cell growth, proliferation, and metabolism.<sup>[2]</sup> Increasing evidence suggests that Rheb and mTORC1 are aberrantly activated in a variety of human cancers.<sup>[3]</sup> The mechanism of mTORC1 activation by Rheb is subject to intense debate.<sup>[4]</sup> K-Ras4B is the most important isoform of the Ras proteins, which hold a central position in the transduction of growth-promoting signals across the plasma membrane to regulate cell growth and differentiation. Mutations in Ras that lead to misregulated signaling are found in approximately 30% of all human cancers.<sup>[5]</sup>

Both Rheb and K-Ras4B contain an S-farnesylated cysteine methyl ester at their C terminus (see Scheme 1). This posttranslational modification is required for their

biological function. Thus, Rheb needs to be farnesylated and methylated for correct localization to endomembranes and for the activation of mTOR kinase,<sup>[3,6,7]</sup> and K-Ras4B needs to be S-farnesylated and carboxymethylated for selective localization to the plasma membrane and signaling activity.<sup>[8]</sup>

For the study of the temporal and spatial organization of Rheb and K-Ras4B in cells, preparative amounts of fully posttranslationally modified and active protein, additionally equipped with suitable reporter groups and tags if required, would be invaluable. The production of such modified proteins by a combination of expression techniques and organic synthesis has proven to be an enabling technique for the study of the S-palmitoylated and S-farnesylated H- and N-Ras proteins and of the S-geranylgeranylated Rab proteins.<sup>[1,9]</sup>

However, farnesylated and carboxymethylated Rheb is not accessible by expression techniques, and, in contrast to the H- and N-Ras proteins, K-Ras4B has not succumbed to synthesis so far. In particular, the maleimide ligation that was very successful for the synthesis of H- and N-Ras<sup>[9]</sup> cannot be applied to K-Ras4B owing to the presence of multiple C-terminal lysine residues and the formation of inseparable product mixtures, and the use of the hydrazide linker employed previously in the synthesis of H- and N-Ras proteins resulted in only low yields of K-Ras4B peptides.<sup>[10]</sup>

Herein we report the first synthesis of S-farnesylated Rheb and K-Ras4B methyl ester by a combination of expressed protein ligation (EPL) and lipopeptide synthesis. In EPL, a recombinant protein thioester generated by thiolysis of an intein fusion protein reacts with a synthetic peptide containing an N-terminal cysteine residue to yield a native amide bond.<sup>[11]</sup>

For the efficient synthesis of Rheb by EPL, the Ala173–Ala174 bond in the C-terminal flexible region<sup>[12]</sup> was chosen as the ligation site. Thus, a farnesylated peptide methyl ester **2** representing the Rheb<sup>174–181</sup> fragment in which Ala174 has been exchanged for Cys174 was required for the synthesis of Rheb, as well as a truncated Rheb $\Delta$ 11 thioester **3** (Scheme 1 a).

Because of the acid sensitivity of the farnesyl group and to ensure that the C-terminal cysteine methyl ester was introduced without epimerization of the activated amino acid to which it needed to be attached, we anchored the peptide to an acid-sensitive trityl resin through the side-chain hydroxy group of Ser180 (Scheme 2). After selective removal of the allyl ester and coupling of the S-farnesylated cysteine methyl

[\*] Dr. Y. Chen,<sup>[4]</sup> Dr. S. Koch,<sup>[4]</sup> Dr. D. Das, Dr. G. Triola, Prof. Dr. H. Waldmann  
Abteilung Chemische Biologie  
Max-Planck-Institut für molekulare Physiologie  
Otto-Hahn-Strasse 11, 44227 Dortmund (Germany)  
and

Fachbereich Chemische Biologie, Fakultät Chemie  
Technische Universität Dortmund  
Otto-Hahn-Strasse 6, 44227 Dortmund (Germany)  
Fax: (+49) 231-133-2499  
E-mail: herbert.waldmann@mpi-dortmund.mpg.de

Dr. K. Uhlenbrock,<sup>[4]</sup> Dr. L. Gremer, Prof. Dr. A. Wittinghofer  
Abteilung Strukturelle Biologie  
Max-Planck-Institut für molekulare Physiologie (Germany)

Dr. K. Weise, Prof. Dr. R. Winter  
Physikalische Chemie I  
Technische Universität Dortmund (Germany)

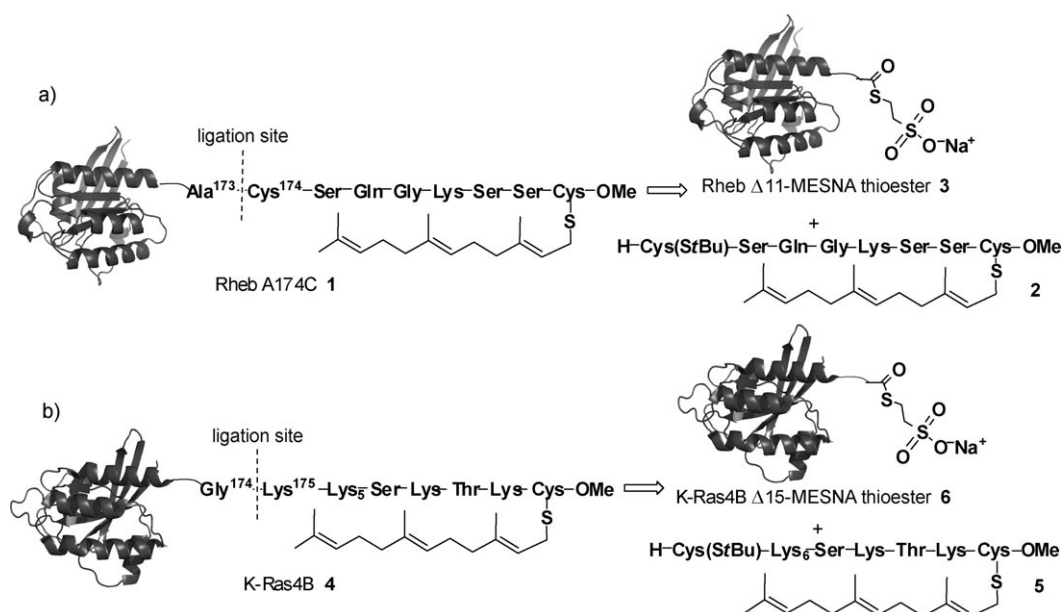
Prof. Dr. L. Brunsveld  
Biomedical Engineering, Laboratory of Chemical Biology  
Eindhoven University of Technology (The Netherlands)

[†] These authors contributed equally to this work.

[\*\*] This research was supported by the Max-Planck-Gesellschaft, the Fonds der Chemischen Industrie, the DFG (SFB 642), and the Alexander von Humboldt-Stiftung. We are grateful to Dr. C. Goemans and Prof. Dr. R. Heumann for providing DNA templates of Rheb, and C. Nowak for technical assistance.



Supporting information for this article is available on the WWW under <http://dx.doi.org/10.1002/anie.201001884>.



**Scheme 1.** Strategy for the synthesis of posttranslationally modified a) Rheb and b) K-Ras4B by EPL. MESNA = mercaptoethanesulfonic acid sodium salt.

ester **10**, the peptide chain was elongated by means of the Fmoc strategy with *N*-Fmoc-protected amino acids containing acid-labile side-chain protecting groups, such as methyltrityl (Mtt) for lysine and trityl (Trt) for serine. The N-terminal cysteine residue was introduced with the thiol group protected as an *S*-*tert*-butyl disulfide, which can be cleaved by reducing reagents before ligation. Finally, treatment of the resin with 1% TFA and a scavenger released the desired peptide **2**, with simultaneous cleavage of all acid-sensitive side-chain protecting groups and without affecting the farnesyl group. After precipitation in diethyl ether, the crude product was purified by HPLC to afford the target peptide in 29% overall yield. The identity and purity of the peptide were confirmed by LC-MS and NMR spectroscopy (see Figures S1 and S2 in the Supporting Information).

To prepare the required protein thioester **3**, we cloned the gene coding for truncated Rheb<sup>1–173</sup> into the IMPACT (intein-mediated purification with an affinity chitin-binding tag) vector pTWIN1 (New England Biolabs).<sup>[13]</sup> The resulting plasmid was transformed into *Escherichia coli* BL21 (DE3) cells, and the recombinant fusion protein Rheb $\Delta$ 11-intein-CBD was purified by chitin-affinity column chromatography. Finally, the desired thioester was released from the column by thiolysis through treatment with MESNA to yield the Rheb $\Delta$ 11-MESNA thioester **3**, which was further purified by size-exclusion chromatography and characterized by ESIMS (see Figure S3 in the Supporting Information). Generally, a quantity of approximately 25 mg of the protein thioester was obtained from a cell-suspension volume of 5 L.

Next, the N-terminal cysteine residue of octapeptide **2** was reduced with tris(2-carboxyethyl)phosphane (TCEP) to demask the thiol group and then ligated with the Rheb $\Delta$ 11-MESNA thioester **3** in the presence of the detergent cetyltrimethylammonium bromide (CTAB),<sup>[9e]</sup> which was

used to drive the ligation reaction to completion within 3 hours (Figure 1a). After precipitation and refolding of the ligation product by pulse dilution into refolding buffer,<sup>[9e]</sup> size-exclusion chromatography yielded soluble protein in 20% yield (Figure 1b). Each ligation reaction can provide Rheb lipoprotein in multi-milligram amounts.

We investigated the ligation product by far-UV CD spectroscopy to verify that it had the correct secondary structure.<sup>[14]</sup> Since the C-terminal

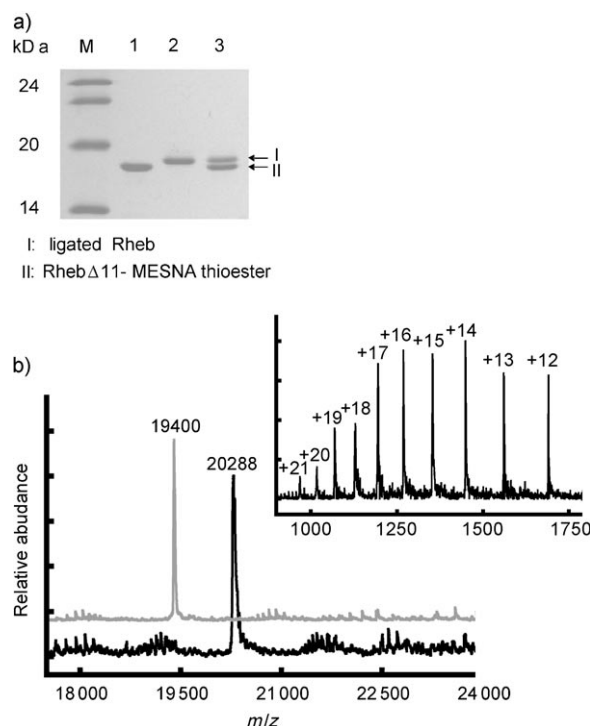
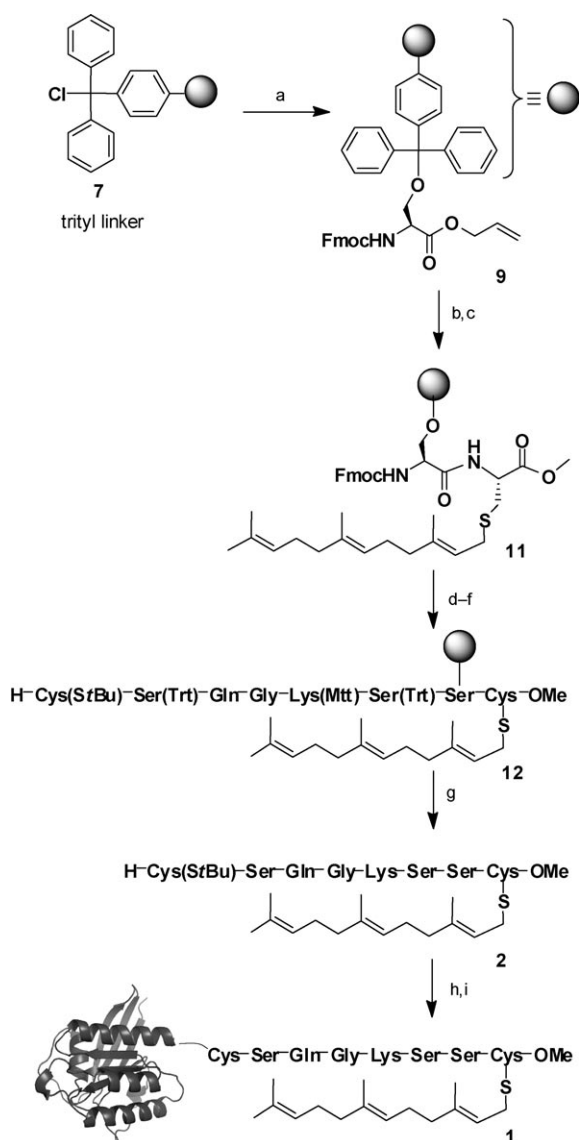


**Figure 1.** Characterization of the product obtained from the ligation of the Rheb $\Delta$ 11-MESNA thioester **3** with the C-terminal octapeptide **2**. a) SDS-PAGE analysis of the Rheb $\Delta$ 11-MESNA thioester (lane 1) and the ligation product obtained after incubation with octapeptide **2** for 3 h (lane 2). Lane 3 contains a mixture of the samples from lanes 1 and 2. b) ESIMS spectra of the purified Rheb lipoprotein **1** ( $M_{\text{calcd}} = 20280$ ) and the Rheb $\Delta$ 11-MESNA thioester **3** ( $M_{\text{calcd}} = 19406$ ). The inset shows the original mass spectrum of the Rheb lipoprotein **1** before deconvolution.



**Scheme 2.** Synthesis of the farnesylated and carboxymethylated Rheb protein **1**. a) Fmoc-Ser-OAll (**8**), pyridine, DMF/CH<sub>2</sub>Cl<sub>2</sub>; b) [Pd(PPh<sub>3</sub>)<sub>4</sub>], PhSiH<sub>3</sub>, CH<sub>2</sub>Cl<sub>2</sub>; c) H-Cys(Far)-OMe (**10**), HATU, collidine, DMF/CH<sub>2</sub>Cl<sub>2</sub>; d) **1**) piperidine in DMF; **2**) Fmoc-AA-OH, HCTU, DIPEA, DMF; AA = Ser(Trt), Lys(Mtt), Gly; repeat; e) **1**) piperidine in DMF; **2**) Fmoc-AA-OH, PyBOP, DIPEA, DMF; AA = Gln, Ser(Trt); repeat; f) **1**) piperidine in DMF; **2**) Fmoc-Cys(SfBu)-OH, PyBOP, collidine, DMF/CH<sub>2</sub>Cl<sub>2</sub>; g) TFA, TES, CH<sub>2</sub>Cl<sub>2</sub>; 29% overall yield from **11**; h) TCEP, ligation buffer; i) RhebΔ11-MESNA thioester **3**, Tris-HCl buffer, pH 7.4, MESNA, CTAB, 20% yield. All = allyl, DIPEA = *N,N'*-diisopropylethylamine, DMF = dimethylformamide, Far = farnesyl, Fmoc = 9-fluorenylmethoxycarbonyl, HATU = 2-(7-aza-1*H*-benzotriazol-1-yl)-1,1,3,3-tetramethyluronium hexafluorophosphate, HCTU = (2-(6-chloro-1*H*-benzotriazol-1-yl)-1,1,3,3-tetramethylammonium hexafluorophosphate), PyBOP = (benzotriazol-1-yloxy)trispyrrolidinophosphonium hexafluorophosphate, TES = triethylsilane, TFA = trifluoroacetic acid, Tris = 2-amino-2-hydroxymethylpropane-1,3-diol.

residues of Rheb are highly flexible and do not determine the overall secondary structure,<sup>[12]</sup> we used the recombinant RhebΔ11-MESNA thioester **3** as a reference for comparison with the structure of the refolded Rheb lipoprotein **1**. The CD spectra of both proteins superimpose very well (Figure 2a),

which indicates that the refolded Rheb lipoprotein and the recombinant Rheb protein adopt a similar secondary structure.

To determine the functionality of the semisynthetic Rheb lipoprotein, we monitored its binding to an effector that inhibits the dissociation of nucleotides from the Ras-like G protein. This interaction can be followed in a real-time fluorescence-based guanine nucleotide dissociation inhibition (GDI) assay,<sup>[15]</sup> which indicates a conformational switch of the G protein between different nucleotide-loaded states. Semisynthetic Rheb lipoprotein was fully loaded with fluorescently labeled methylantraniloyl (mant) nucleotides (i.e. mant-GppNHp, a nonhydrolysable GTP analogue, or the analogous mant-GDP). Upon the addition of excess unlabeled nucleotides (GppNHp or GDP), the bound mant nucleotides are exchanged for unlabeled nucleotides. Since the fluorescence intensity of the Rheb-bound mant nucleotide is approximately twice as high as the fluorescence intensity of the free mant nucleotide, the nucleotide-exchange reaction can be monitored as decay of the fluorescence signal. Recombinant forms of possible Rheb effectors, such as mTOR itself or the mTORC1 complex, are not known. However, we recently developed a mutated form of the Ras binding domain of the Raf protein (Raf-RBD) that specifically recognizes GTP-bound Rheb and therefore inhibits the dissociation of the nucleotide from active Rheb.<sup>[16]</sup> We applied both wild-type and mutated Raf-RBD proteins to active (mant-GppNHp-loaded) or inactive (mant-GDP-loaded) semisynthetic Rheb lipoprotein in the GDI assay. In the presence of mutated Raf-RBD, the nucleotide exchange of mant-GppNHp-bound Rheb was slowed down, whereas in the presence of wild-type Raf-RBD, there was no change relative to the intrinsic rate (Figure 2b). In contrast, for mant-GDP-bound Rheb, neither mutated nor wild-type Raf-RBD affected the rate of the nucleotide-exchange reaction. These results prove that the semisynthetic Rheb lipoprotein was correctly folded and functional, as indicated by conformational switching between the active and the inactive state.

The K-Ras4B protein **4** was synthesized by a similar strategy (Scheme 1b). K-Ras4B also does not contain an extra cysteine residue at its C terminus for protein ligation. In this case, a cysteine residue was inserted at the N-terminal end of the polybasic amino acid sequence adjacent to the farnesylated C-terminal cysteine methyl ester. The resulting dodecapeptide **5**, which features a total of eight lysine residues, was synthesized on a solid support (see Scheme S1 in the Supporting Information). The growing peptide chain was anchored to a chlorotriyl linker through the side chain of the lysine residue nearest the C terminus. The other lysine side chains were protected with the allyloxycarbonyl (Alloc) group<sup>[17]</sup> to enable their orthogonal palladium(0)-catalyzed deprotection in the presence of the other functionalities in the peptide. After cleavage from the solid support, the peptide could be precipitated readily and was obtained in 15% overall yield after preparative HPLC purification. Similarly to the Rheb thioester **3**, the truncated K-Ras4B protein core thioester **6** was generated through expression in the IMPACT vector pTWIN2 (New England Biolabs), purification on a chitin-affinity column, and release after treatment

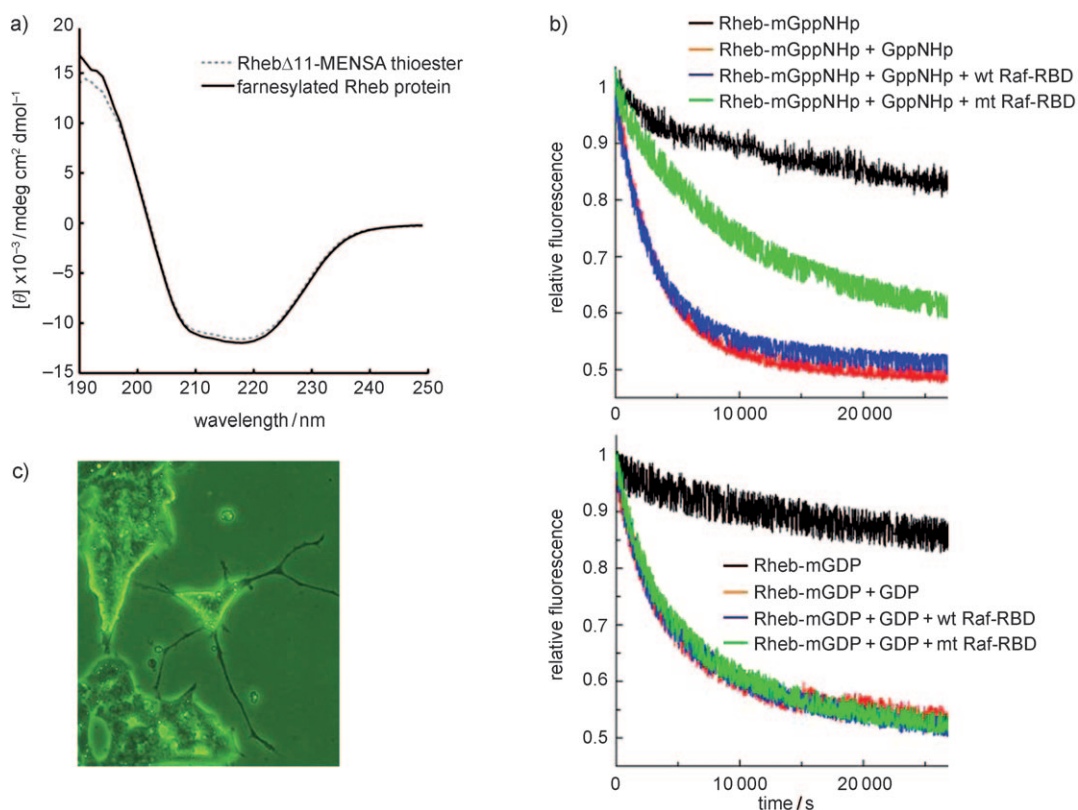


**Figure 2.** Evidence for the correct function of the synthetic Rheb and K-Ras4B lipoproteins. a) CD spectra of the recombinant Rheb $\Delta$ 11-MESNA thioester **3** (.....) and the Rheb lipoprotein **1** (—) in 20 mM phosphate buffer (pH 7.2). b) GDI assay showing the release of mant-labeled nucleotides (mant-GppNHp or mant-GDP) from Rheb lipoprotein in the presence or absence of wild-type (wt) Raf-RBD or mutated (mt) Raf-RBD upon the addition of excess unlabeled nucleotides (GppNHp or GDP). c) Microscopy image showing the neuritelike outgrowth of PC12 cells following the microinjection of semisynthetic farnesylated G12VK-Ras4B. The total number of cells injected with the protein in three independent experiments was 39; 10 cells in experiment 1, 20 cells in experiment 2, and 9 cells in experiment 3. A 200  $\mu$ M protein solution containing FITC-dextran (20 mM) was used for microinjections.

with MESNA. The synthetic farnesylated polybasic peptide **5** was ligated to the K-Ras4B thioester **6** in Tris buffer in the presence of TCEP (5 mM) to yield the ligated K-Ras4B protein **4**, which contains an additional cysteine residue between Gly174 and Lys175, within 4 hours with up to 80% conversion and in multi-milligram amounts (see Figure S5 in the Supporting Information).

In contrast to the Rheb protein, protein denaturation and refolding was not necessary for the purification of K-Ras4B. In this case, the different physical properties of the ligated K-Ras4B protein (isoelectric point, pI=8.2) and the core protein (pI=5.3) enabled an efficient purification by cation-exchange chromatography to yield K-Ras4B in 50–70% yield.

To demonstrate the molecular integrity and biological activity of the farnesylated K-Ras4B protein, we prepared an oncogenic G12VK-Ras4B $\Delta$ 15 MESNA thioester and ligated it to the K-Ras4B dodecapeptide **5**. This semisynthetic construct was then investigated for its ability to induce differentiation of the rat pheochromocytoma PC12 cell line (see Table S1 in the Supporting Information).<sup>[9]</sup> Under normal growth conditions, this cell line has a chromaffin-cell-like morphology. Upon the microinjection of a 200  $\mu$ M solution of full-length recombinant oncogenic K-RasG12V protein, 69% of these cells differentiated into nonreplicating sympa-

thetic neuronlike cells. Similarly, upon the microinjection of a 100  $\mu$ M solution of semisynthetic oncogenic K-Ras4B, 57% of the treated cells showed neurite outgrowth; 67% activity was observed when the cells were injected with a 200  $\mu$ M solution (Figure 2c).

Correctly modified and functional Rheb **1** and K-Ras4B **4** may be employed as tools to investigate the roles of the proteins in biological processes, for example, their interaction with putative binding partners. To demonstrate this possibility, we investigated whether the semisynthetic lipoproteins interact with the  $\delta$  subunit of retinal rod phosphodiesterase (PDE $\delta$ ). PDE $\delta$  has been suggested to be a transport factor for prenylated proteins.<sup>[18]</sup>

PDE $\delta$  can recognize the prenyl group of these proteins; however, the range of its binding partners and the structural parameters dictating this protein–protein interaction remain to be defined.<sup>[18,19]</sup> Hence, we subjected the semisynthetic Rheb and K-Ras4B lipoproteins loaded with mant-GppNHp, as well as several truncated model peptides labeled with a dansyl group, to a fluorescence-polarization assay to determine their binding affinity for PDE $\delta$  (Table 1).

The semisynthetic Rheb and K-Ras4B proteins did interact with PDE $\delta$ ; they showed similar  $K_D$  values of 394 and 302 nM, respectively. By contrast, a recombinant Rheb

**Table 1:** Interaction of farnesylated Rheb and K-Ras4B, as well as several dansylated C-terminal peptides derived from these proteins, with PDE $\delta$ , as determined by fluorescence-polarization assays.

Protein/peptide	$K_D$ [nM]
Rheb mant-GppNHp	394
K-Ras4B mant-GppNHp	302
dansyl-GKSSC(Far)-OMe ( <b>13</b> ; from Rheb)	102
H-Cys(S $\dagger$ Bu)K(Dan)K <sub>5</sub> SKTKC(Far)-OMe <sup>[a]</sup> ( <b>14</b> ; from K-Ras4B)	227
dansyl-GC(Far)-OMe ( <b>15</b> )	616
dansyl-GK <sub>3</sub> SC(GerGer)-OMe ( <b>16</b> ; from Rap1A)	> 10000

[a] Dan = dansyl.

protein lacking the farnesyl group displayed no interaction with PDE $\delta$  (data not shown). To study this interaction in more detail, we synthesized several dansylated peptides corresponding to truncated C termini of the Rheb protein **13** and K-Ras4B protein **14**, as well as an S-geranylgeranylated peptide **16** derived from Rap1A and a dipeptide **15** containing a farnesylated cysteine methyl ester, and investigated their affinity for PDE $\delta$ . Whereas the farnesylated dipeptide **15** showed a  $K_D$  value of 616 nM, the C termini of Rheb and K-Ras4B displayed increased affinity, with  $K_D$  values of 102 and 227 nM, respectively. In contrast, the geranylgeranylated C terminus of Rap1A, **16**, showed a weak interaction with PDE $\delta$ . This result confirmed that PDE $\delta$  is not a general prenyl-binding protein, but selectively binds farnesylated proteins.<sup>[19]</sup> These findings indicate that a farnesylated C terminus is required, but not sufficient, for high-affinity binding to PDE $\delta$ , and that the C-terminal amino acid sequence influences binding significantly. Binding is modulated by the protein core only to a smaller extent. These results also strongly support the finding that PDE $\delta$  is able to solubilize both Ras proteins and Rheb in live cells.<sup>[16]</sup>

To further demonstrate the usefulness of the semisynthetic lipoproteins as probes, we investigated the distribution of K-Ras4B into different membrane subdomains. For K-Ras4B it has been proposed that the membrane anchor composed of the farnesyl group and the polybasic amino acid stretch leads to an accumulation of the protein in liquid-disordered membrane subdomains.<sup>[20]</sup> For N-Ras proteins we showed recently that their dual-lipid S-palmitoyl/S-farnesyl anchor induces accumulation of the proteins in the liquid-ordered/liquid-disordered ( $l_o/l_d$ ) domain interface.<sup>[21,22]</sup> The lateral segregation of a protein with a membrane anchor composed of a farnesyl group and a polybasic amino acid stretch has not been studied previously. Therefore, we analyzed the interaction of the farnesylated K-Ras4B with lipid domains of negatively charged heterogeneous model membranes by tapping-mode atomic force microscopy (AFM). An appropriate system for analysis was produced by complementing the neutral zwitterionic canonical raft mixture DOPC/DPPC/Chol 1:2:1 with negatively charged lipids. This approach was based on the fact that the positively charged lysine residues in the K-Ras4B membrane-anchor region strongly interact with negatively charged lipids. The incorporation of 10 mol % negatively charged phosphatidylglycerol still leads to segregation into  $l_o$  and  $l_d$  domains. A concentration of anionic lipids of 10 % is within the typical physiological range.<sup>[23,24]</sup>

AFM measurements were performed by the technique of direct injection of the protein-containing solution into the AFM fluid cell to enable imaging of the same sample area before and after incorporation of the protein. The AFM image before the addition of K-Ras4B showed a homogeneous DOPC/DOPG/DPPC/DPPG/Chol (20:5:45:5:25) lipid bilayer with isolated islands of fluid  $l_d$  domains (dark brown, Figure 3 a) in a coherent pool of a raftlike ( $l_o$ ) protruding phase (light brown). The thickness of the lipid bilayer was 5.2 nm for the  $l_o$  phase and 4.0 nm for the  $l_d$  phase; that is, the coexisting phases could be clearly distinguished by a height difference of approximately 1.0 nm (Figure 3 c), in agreement with previous results.<sup>[21]</sup> After the addition of K-Ras4B protein, the AFM measurements indicated the exclusive localization of K-Ras4B in the bulk  $l_d$  phase of the membrane (Figure 3 b). The protein exhibited a mean height of  $(2.0 \pm 0.7)$  nm (mean value  $\pm$  standard deviation,  $n = 304$ ; Figure 3 d), which corresponds well to the linear dimension of a K-Ras4B molecule.

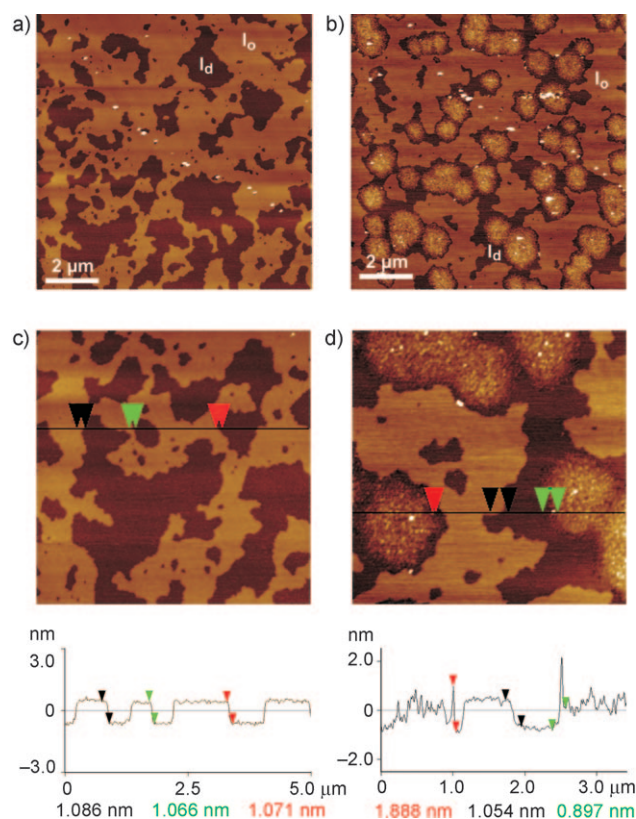


**Figure 3.** AFM images of the partitioning of the K-Ras4B lipoprotein into anionic lipid bilayers consisting of DOPC/DOPG/DPPC/DPPG/Chol (20:5:45:5:25; molar ratio). The AFM images are shown a) before and b) after injection of K-Ras4B into the AFM fluid cell. c,d) Lower left-hand areas of AFM images (a) and (b), respectively, at higher magnification, and section profiles along the horizontal black lines in the images. The vertical color scale in the AFM images from dark brown to white corresponds to an overall height between 6 and 5 nm, respectively. The vertical distances between pairs of arrows (black, green, and red) are given in the corresponding color below the graphs. Chol = cholesterol, DOPC = 1,2-dioleoyl-*sn*-glycero-3-phosphocholine, DOPG = 1,2-dioleoyl-*sn*-glycero-3-phospho(1'-*rac*-glycerol), DPPC = 1,2-dipalmitoyl-*sn*-glycero-3-phosphocholine, DPPG = 1,2-dipalmitoyl-*sn*-glycero-3-phospho-(1'-*rac*-glycerol) sodium salt.

Whereas N-Ras proteins with at least one farnesyl anchor showed a time-dependent diffusion and subsequent clustering in the  $l_o/l_d$  phase-boundary region,<sup>[21]</sup> the formation of new domains with accumulated protein inside a fluidlike environment was observed for the farnesylated K-Ras4B protein. These new domains enriched in K-Ras4B had a thickness ( $0.9 \pm 0.1$ ) nm ( $n = 119$ ) larger than that of the fluid lipid phase (Figure 3d) and were stable over the whole time range covered. In contrast to the distribution observed for the neutral C terminus of N-Ras, in the case of the K-Ras4B protein the strong electrostatic interaction between its positively charged lysine residues and the negatively charged lipid headgroups of the membrane seems to control the partitioning behavior, whereby the bulky farnesyl anchor prevents the partitioning of K-Ras4B into ordered raftlike domains. Interestingly, insertion into the fluidlike lipid phase with 5% anionic headgroups is also not energetically very favorable. As a consequence, further anionic lipids are recruited, probably by an effective lipid-sorting mechanism, and new fluid domains with a higher anionic charge density and greater amounts of incorporated protein are formed. These observations are in agreement with the proposal originating from experiments with live cells that polybasic K-Ras4B organizes into specific microdomains distinct from classical lipid rafts in plasma membranes.

In conclusion, we have described the synthesis of preparative amounts of fully posttranslationally modified Rheb and K-Ras4B proteins. The functionality of these semisynthetic proteins was demonstrated by means of biochemical, biophysical, and cell-based methods. Our results demonstrate that the semisynthetic, fully modified proteins may be employed as invaluable tools for the study of Rheb and K-Ras4B proteins in cells.

Received: March 30, 2010

Published online: July 22, 2010

**Keywords:** expressed protein ligation · fluorescence spectroscopy · lipoproteins · scanning probe microscopy · solid-phase synthesis

- [1] a) M. H. Gelb, L. Brunsveld, C. A. Hrycyna, S. Michaelis, F. Tamanoi, W. C. Van Voorhis, H. Waldmann, *Nat. Chem. Biol.* **2006**, *2*, 518–528; b) L. Brunsveld, J. Kuhlmann, K. Alexandrov, A. Wittinghofer, R. S. Goody, H. Waldmann, *Angew. Chem.* **2006**, *118*, 6774–6798; *Angew. Chem. Int. Ed.* **2006**, *45*, 6622–6646; c) Y. Takai, T. Sasaki, T. Matozaki, *Physiol. Rev.* **2001**, *81*, 153–208; d) A. Wittinghofer, H. Waldmann, *Angew. Chem.* **2000**, *112*, 4360–4383; *Angew. Chem. Int. Ed.* **2000**, *39*, 4192–4214; e) M. Barbacid, *Annu. Rev. Biochem.* **1987**, *56*, 779–827.
- [2] a) P. Polak, M. N. Hall, *Curr. Opin. Cell Biol.* **2009**, *21*, 209–218; b) X. J. M. Ma, J. Blenis, *Nat. Rev. Mol. Cell Biol.* **2009**, *10*, 307–318; c) J. Avruch, K. Hara, Y. Lin, M. Liu, X. Long, S. Ortiz-Vega, K. Yonezawa, *Oncogene* **2006**, *25*, 6361–6372; d) P. J. Aspuria, F. Tamanoi, *Cell. Signalling* **2004**, *16*, 1105–1112.
- [3] A. B. Hanker, N. Mitin, R. S. Wilder, E. P. Henske, F. Tamanoi, A. D. Cox, C. J. Der, *Oncogene* **2010**, *29*, 380–391.
- [4] a) T. Sato, A. Nakashima, L. Guo, F. Tamanoi, *J. Biol. Chem.* **2009**, *284*, 12783–12791; b) K. Uhlenbrock, M. Weiwad, R. Wetzker, G. Fischer, A. Wittinghofer, I. Rubio, *FEBS Lett.* **2009**, *583*, 965–970; c) Y. Sun, Y. Fang, M. S. Yoon, C. Zhang, M. Rocco, F. J. Zwartkruis, M. Armstrong, H. A. Brown, J. Chen, *Proc. Natl. Acad. Sci. USA* **2008**, *105*, 8286–8291; d) X. C. Bai, D. Z. Ma, A. L. Liu, X. Y. Shen, Q. J. M. Wang, Y. J. Liu, Y. Jiang, *Science* **2007**, *318*, 977–980.
- [5] J. L. Bos, *Cancer Res.* **1989**, *49*, 4682–4689.
- [6] K. Takahashi, M. Nakagawa, S. G. Young, S. Yamanaka, *J. Biol. Chem.* **2005**, *280*, 32768–32774.
- [7] C. Buerger, B. DeVries, V. Stambolic, *Biochem. Biophys. Res. Commun.* **2006**, *344*, 869–880.
- [8] a) J. F. Hancock, *Nat. Rev. Mol. Cell Biol.* **2003**, *4*, 373–384; b) J. F. Hancock, R. G. Parton, *Biochem. J.* **2005**, *389*, 1–11; c) O. Rocks, A. Peyker, P. I. H. Bastiaens, *Curr. Opin. Cell Biol.* **2006**, *18*, 351–357; d) J. Omerovic, A. J. Laude, I. A. Prior, *Cell. Mol. Life Sci.* **2007**, *64*, 2575–2589; e) S. Eisenberg, Y. I. Henis, *Cell. Signalling* **2008**, *20*, 31–39.
- [9] For selected references on lipopeptide and lipoprotein synthesis see: a) E. Nägele, M. Schelhaas, N. Kuder, H. Waldmann, *J. Am. Chem. Soc.* **1998**, *120*, 6889–6902; b) K. Kuhn, D. J. Owen, B. Bader, A. Wittinghofer, J. Kuhlmann, H. Waldmann, *J. Am. Chem. Soc.* **2001**, *123*, 1023–1035; c) B. Bader, K. Kuhn, D. J. Owen, H. Waldmann, A. Wittinghofer, J. Kuhlmann, *Nature* **2002**, *403*, 223–226; d) K. Alexandrov, I. Heinemann, T. Durek, V. Sidorovitch, R. S. Goody, H. Waldmann, *J. Am. Chem. Soc.* **2002**, *124*, 5648–5649; e) T. Durek, K. Alexandrov, R. S. Goody, A. Hildebrand, I. Heinemann, H. Waldmann, *J. Am. Chem. Soc.* **2004**, *126*, 16368–16378; f) G. Kragol, M. Lumbierres, J. M. Palomo, H. Waldmann, *Angew. Chem.* **2004**, *116*, 5963–5966; *Angew. Chem. Int. Ed.* **2004**, *43*, 5839–5842; g) D. Gottlieb, C. Grunwald, C. Nowak, J. Kuhlmann, H. Waldmann, *Chem. Commun.* **2006**, 260–262.
- [10] H. Waldmann, S. Koch, unpublished results.
- [11] R. R. Flavell, T. W. Muir, *Acc. Chem. Res.* **2009**, *42*, 107–116.
- [12] Y. D. Yu, S. Li, X. Xu, Y. Li, K. L. Guan, E. Arnold, J. P. Ding, *J. Biol. Chem.* **2005**, *280*, 17093–17100.
- [13] T. C. Evans, J. Benner, M. Q. Xu, *Protein Sci.* **1998**, *7*, 2256–2264.
- [14] S. R. Martin, P. M. Bayley, *Methods Mol. Biol.* **2002**, *173*, 43–55.
- [15] M. R. Ahmadian, A. Wittinghofer, C. Herrmann, *Methods Mol. Biol.* **2002**, *189*, 45–63.
- [16] K. Uhlenbrock, A. Wittinghofer, unpublished results.
- [17] H. Kunz, C. Unverzagt, *Angew. Chem.* **1984**, *96*, 426–427; *Angew. Chem. Int. Ed. Engl.* **1984**, *23*, 436–437.
- [18] V. Nancy, I. Callebaut, A. El Marjou, J. de Gunzburg, *J. Biol. Chem.* **2002**, *277*, 15076–15084.
- [19] H. B. Zhang, X. H. Liu, K. Zhang, C. K. Chen, J. M. Frederick, G. D. Prestwich, W. Baehr, *J. Biol. Chem.* **2004**, *279*, 407–413.
- [20] a) I. A. Prior, C. Muncke, R. G. Parton, J. F. Hancock, *J. Cell Biol.* **2003**, *160*, 165–170; b) S. J. Plowman, N. Ariotti, A. Goodall, R. G. Parton, J. F. Hancock, *Mol. Cell Biol. Res. Commun.* **2008**, *28*, 4377–4385.
- [21] K. Weise, G. Triola, L. Brunsveld, H. Waldmann, R. Winter, *J. Am. Chem. Soc.* **2009**, *131*, 1557–1564.
- [22] A. Vogel, G. Reuther, K. Weise, G. Triola, J. Nikolaus, K.-T. Tan, C. Nowak, A. Herrmann, H. Waldmann, R. Winter, D. Huster, *Angew. Chem.* **2009**, *121*, 8942–8945; *Angew. Chem. Int. Ed.* **2009**, *48*, 8784–8787.
- [23] G. B. Díaz, A. M. Cortizo, M. E. Garcia, J. J. Gagliardino, *Lipids* **1988**, *23*, 1125–1128.
- [24] D. A. White, *The Phospholipid Composition of Mammalian Tissues*, Vol. 3, 2nd ed., Elsevier, New York, **1973**.